Asian Journal of Chemistry; Vol. 28, No. 8 (2016), 1697-1702

ASIAN JOURNAL OF CHEMISTRY

http://dx.doi.org/10.14233/ajchem.2016.19791

Preparation, Characterization and Activity of Ni and N co-doped TiO_2 Photocatalyst in Degradation of Methylene Blue

S. PRIATMOKO[1,2,*], TRIYONO[2], I. KARTINI[2] and ROTO[2]

[1]Department of Chemistry, Semarang State University, Semarang, Indonesia
[2]Department of Chemistry, Universitas Gadjahmada, Yogyakarta, Indonesia

*Corresponding author: Fax: +62 24 8508035; Tel: +62 81 57779641; Email: sigit_chemunnes@yahoo.com; sigitwarsono@mail.unnes.ac.id

Received: 23 December 2015; *Accepted*: 2 February 2016; *Published online*: 30 April 2016; AJC-17875

Preparation of Ni and N co-doped TiO_2 photocatalyst using sol-gel method with precursors titanium isobutoxide, nickel nitrate and urea, respectively as a source of titanium, nickel and nitrogen have been done. Photocatalyst were characterized using X-ray diffraction, spectroscopy UV-visible diffuse reflectance, scanning electron microscopy, FTIR spectroscopy. Photocatalytic activity was tested against the degradation of methylene blue using visible light from xenon lamp 300 watt. The results showed that on the TiO_2 co-doped Ni and N indicates that encouragement the concentration of Ni (at fixed concentration of N), causing an increase in crystallite size. While on boosts concentration N (at fixed concentrations of Ni) initially provides enhanced crystallite size and reaches a maximum at certain composition. Addition of a single dopant Ni and N decrease the band gap energy of TiO_2 and obtained the lowest value of each successive 3.080 and 3.093 eV. The addition of double dopant Ni and N are generally lowers the band gap energy of TiO_2. The activity of the Ni-N-TiO_2 photocatalyst showed the optimum time degradation in the 90th min with a degradation rate of approximately 80 % obtained in the photocatalyst with composition % mol ratio of Ni:N = 2.5: 2.5.

Keywords: Photocatalyst, TiO_2, Doped, Degradation, Methylene blue.

INTRODUCTION

One important photocatalyst material that is widely used in photocatalytic wastewater treatment is titanium dioxide (TiO_2) or titania [1-3]. Several factors are the reason why the TiO_2 is widely used as an object of study photocatalytic reaction interesting: it has high stability, has a band gap energy of a moderate, non-toxic and has a high surface area [3-5]. As an n-type semiconductor, titania has 3 different polymorphs are: anatase, rutile and brookite with successive band gap energy are 3.2, 3 and 3.05 eV, respectively [6]. On the dimensions of extremely small particles, the surface energy is an important part of the overall energy system and found that anatase has the lowest surface energy than the rutile phase and brookite [6,7]. For this reason anatase widely used as a photocatalyst. Nevertheless, anatase has the disadvantage of having energy band gap energy is large enough, so that the solar radiation that contains only ultra-violet waves about 3-4 %, not able to activate the photocatalyst. Therefore it is necessary to modify the structure of the band gap energy anatase in order to work in the wavelength region of visible light.

One method that can be used to modify the band gap energy of TiO_2 is by doping metals and non-metals to the surface of the photocatalyst [8]. The existence of dopants in a photocatalyst TiO_2 can cause a significant shift to the absorption of visible light compared to pure photocatalysts [9] because the dopants can change the electronic structure of the photocatalyst so as to alter the responsiveness of TiO_2 to visible light. A dopant can also work as an electron trap that leads from charge carriers generated and minimize recombination between holes with electrons. Doping TiO_2 using transition metal ions and non-metallic elements have done some research [10-12]. Transition metal ions are often used as a doping agent because it has a strong ability to absorb visible light and generally have ionic radii similar to titanium ions [13]. The use of nitrogen dopant into the TiO_2 structures have been reported by Viswanathan and Krishnamurthy [14] that synthesize N-TiO_2 nanoparticles anatasee using sol-gel method. The result is a synthesis of N-TiO_2 has a band gap energy of 1.95 eV, much lower than Degussa P25 TiO_2 band gap energy in the amount of 3.10 eV so as to shift the activity of TiO_2 to visible light region. In this article the use of dual dopant Ni and N in TiO_2 structure using sol-gel method reported. The characteristics of photocatalyst obtained by XRD method, the DR-UV and SEM as well as testing it photocatalytic activity against degradation of methylene blue.

EXPERIMENTAL

Preparation of photocatalyst: Synthesis of Ni-TiO_2 carried out according to the procedures conducted by Zhang and Liu [2] with modifications to the type of precursor N is used, *i.e.* urea and titanium isobutoxide as precursor of TiO_2. Typically, a total of 0.1 mol titanium isobutoxide dissolved in 100 mL of absolute ethanol to form a solution of urea (solution 1). A certain amount of nickel nitrate hexahydrate put in a mixture of 50 mL of deionized water whose pH is set 1.5 with nitric acid and 50 mL ethanol to form a solution 2. Furthermore solution 1 was added dropwise to a solution 2 within 60 min while stirring rapidly at room temperature to form a sol, followed by continuous stirring for 5 h and finally followed by the aging process at room temperature for 3 days to form a gel. The resulting gel product is then dried at 80 °C for 10 h, followed by milling and annealing at temperatures that have been designed (400, 500 and 600 °C) for 2 h to remove organic residues. Results of this process is formation of photocatalyst Ni-N-TiO_2. The samples is then inserted in the air tight chamber until now will be analyzed and used. For the preparation of the doped TiO_2 single Ni and N and TiO_2 without dopants is done by changing the components of the solution 2. For other processes using the same principles as the synthesis of Ni-N-TiO_2. Levels of Ni and N doped TiO_2 in either single or multiple variation which is 2.5 %, 5 % and 10 % mol.

Characterization: The results of preparation Ni-N-TiO_2 photocatalyst as mentioned above were analyzed microstructure properties include the complete phase and crystallinity using X-ray diffraction (XRD). The radiation source used comes from CuK_α (λ = 1,54060Å) with operating conditions voltage 40 kV, current of 30 mA, 2θ angle range between 15° to 80° and a speed of 5° per min observation. All the diffraction pattern of the sample analysis results are then compared standard JCPDS XRD diffraction pattern 841826. anatase of TiO_2 levels can be predicted using the equation suggested by Ganesh *et al.* [15].

$$\text{Anatase } (\%) = \frac{100}{1 + 1.33[I(R)/I(A)]} \quad (1)$$

In this case, I(R) and I(A) are the intensity of rutile and intensity anatase, respectively. The average size of crystallites sampled predicted using Debye-Scherrer equation. Absorption spectra diffusion reflectance UV-visible (DRUV) samples are recorded with a Shimadzu spectrophotometer UV1700 Specular reflectance attachment at room temperature with a scanning range between 200 to 800 nm. The spectral data is used to measure the value of the band gap energy of the sample. Micrograph crystallite morphology and composition of the samples was determined by SEM JEOL JED-2300 equipped with energy dispersive spectroscopy X-ray (EDX). Characterization of functional groups TiO_2, Ni-TiO_2, N-TiO_2 and Ni-N-TiO_2 is done by using an infrared spectrophotometer Shimadzu FTIR Prestige21 at wave number 4000-300 cm^{-1} with KBr pellet method.

Photocatalytic activity: For the purposes of photocatalytic activity test, the sample Ni-N-TiO_2 photocatalyst introduced into the reactor made of Pyrex glass cylinder with a diameter of 8 cm and a height of 10 cm which already contains methylene blue solution. Methylene blue was chosen because it has several characters, strong adsorbed on the surface of metal oxide, both the optical absorption properties and resistance to light degradation [16]. The reactor was then put in a box cube dimensions of 30 cm × 30 cm × 30 cm, air tight and equipped with magnetic stirrer and hotplate and 6000 K xenon lamp 2 × 35 watts as a source of visible light photons. The distance between the lamp with the reactor ± 20 cm. The use of UV light as a photon source also learned that by replacing the xenon lamp with UV light that has a wavelength of 254 nm. At each experiment, a total of 0.25 grams of sample photocatalyst is added to 25 mL of methylene blue 5 ppm. Methylene blue solution and the mixture is then stirred with a photocatalyst samples were exposed for 60 min. Every 15 min measurements Methylene blue concentration in the mixture using a UV-visible spectrophotometer. The amount of degraded methylene blue determined by the equation:

$$\text{Degradation of MB } (\%) = \frac{[MB]_{initial} - [MB]_{final}}{[MB]_{initial}} \times 100 \quad (2)$$

RESULTS AND DISCUSSION

Synthesis and characterization of materials: Diffractogram pattern of TiO_2 photocatalyst synthesized by the temperature variations of 400, 500 and 600 °C are presented in Fig. 1. It appears that the increase in the calcination temperature raises crystallinity and composition of rutile phase TiO_2 structure as well as reported by some researchers [3,4]. Generally, anatase showed higher photocatalytic activity than rutile. Although still debated, one reason is anatase classified as semiconductor indirect that causes age of electron and hole results excitation photon longer than semiconductors for direct transition of electrons from the conduction band to the valence band in the semiconductor [17,18]. Based on Fig. 1, the phase anatase occurred at 400 °C are shown in the peak of the angle 2θ 25.35°; 38.62°; 48.09°; 55.12°; 62.75°; 75.20°. According to Nguyen *et al.* [19] these peaks are a diffraction of region (101), (004), (200), (105), (211) and (204) TiO_2 anatase. Calculations using eqn. 1 shows that levels of anatase at 400 °C for 73 %. Increasing of calcination temperature, as shown in Fig. 1, causing a reduction in TiO_2 anatase phase. This is apparently due to the high temperatures increased migration distribution of Ti^{4+} and O^{2-} into the crystal lattice caused the rearrangement of the structure of TiO_2 thus affecting the distance between Ti and O atoms [12,20]. Further large crystal size can be estimated by using the Debye-Scherrer equation. For each sample, the results are, respectively 13.117 nm (400 °C), 18.2 nm (500 °C) and 37.014 nm (600 °C). It appears that the higher the calcination temperature the larger the particle size and rutile phase. Increasing the particle size leads to reduced photocatalytic activity [21].

Figs. 2 and 3 demonstrate the diffractogram TiO_2 that has been doped with Ni and N (Ni-N-TiO_2). Fig. 2 presents the effect of the addition of dopants Ni (N concentration fixed) to the X-ray diffraction pattern, while Fig. 3 presented to the contrary. Based on these images it appears that a large angle 2θ indicating anatase TiO_2 unchanged despite doped with Ni and N, as described by Nguyen *et al.* [19]. Diffractogram

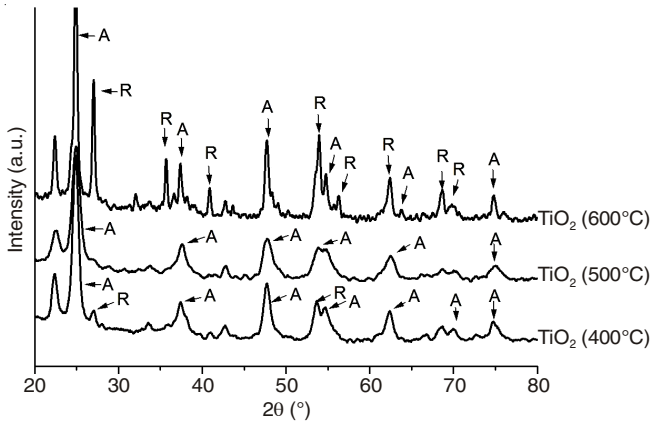

Fig. 1. Diffractogram pattern of TiO_2 samples calcined at 400, 500 and 600 °C

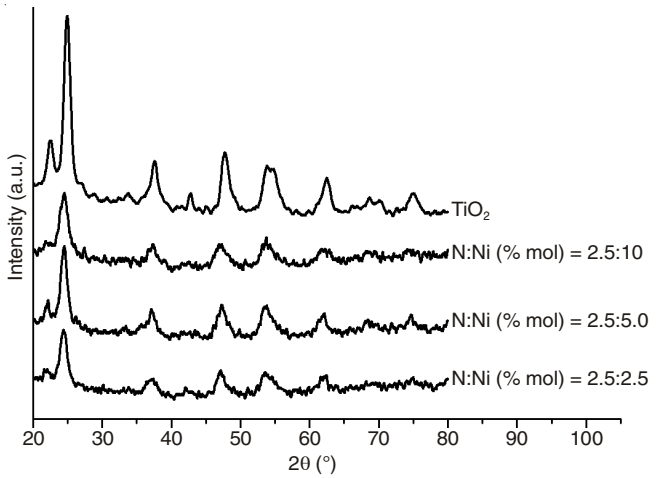

Fig. 2. XRD pattern of pure TiO_2 and TiO_2 co-doped Ni and N at varied concentration of Ni (at N fixed); all the material was calcined at 400 °C

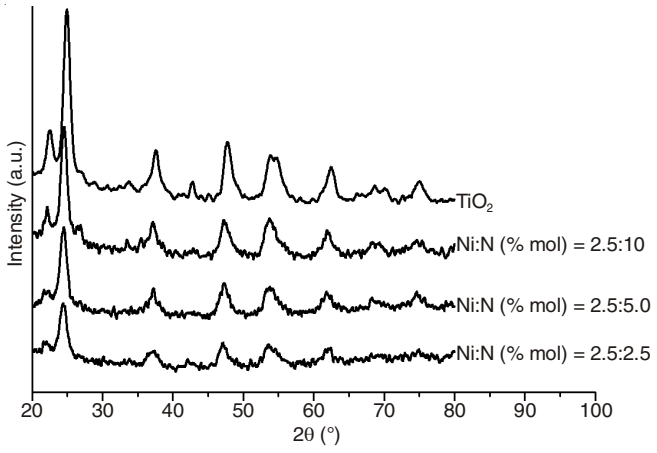

Fig. 3. XRD pattern of pure TiO_2 and TiO_2 co-doped Ni and N at varied concentration of N (at Ni fixed); all the material was calcined at 400 °C

characteristic differences which exist only on the crystallinity of the sample shown by the intensity and width of diffractogram peaks. The diffractogram peaks of Ni and N co-doped TiO_2 samples with concentration of N varied (fixed concentration of Ni) looks sharper when compared with the doped TiO_2 samples of Ni and N with concentration of Ni varied (fixed concentration of N). This means increased concentration of N (at fixed Ni concentration) a greater influence on the crystallinity than increased concentration of Ni (at fixed N concentration). However, increased content of Ni and N in TiO_2 in both sample groups, initially increasing the crystallinity of the sample, but then declined after having reached a certain level. For each group of samples, the peak of the photocatalyst materials diffractogram mol % composition ratio N:Ni = 2.5:5 and 2.5:10 looks sharper when compared with other photocatalyst materials. A decrease in intensity at the peak of TiO_2 anatase probably due to the presence of Ni^{2+} ions into the crystal structure of TiO_2 thus affecting the regularity of crystalline TiO_2. Likewise, the presence of dopant N which also contribute for TiO_2 crystals damage. The existence of peaks in a diffractogram NiO TiO_2 according to Chen *et al*. [22] is located at the corners of 2θ of 37.5° and 44°. Nonetheless, based on the results of research that has been carried out on the entire sample did not show any peak of NiO. Allegedly this is due to the levels of Ni goes into TiO_2 relatively small so if Ni is uniformly distributed on the surface of TiO_2, the concentration of Ni becomes small so as not detected by XRD.

Based on the peak diffractogram of TiO_2 (200) and the calculation using the Debye-Scherrer equation, we can determine the average size of TiO_2 anatase crystallites that have been double doped with Ni and N (Ni-N-TiO_2) as presented in Table-1. From the Table-1 it appears that overall average crystallite size of Ni and N co-doped TiO_2 photocatalyst below 50 nm, indicating that all the results of the synthesis is nano-sized. For fixed N photocatalyst composition (2.5 mol %), increased levels of Ni increase the average size of crystallites. However, the pattern of this trend may be changing with increasing dopant concentration Ni because this research, Ni dopant concentrations are higher has not been conducted. In contrast to the photocatalyst with fixed composition of Ni (2.5 % mol), enhance the concentration of dopant N initially provides enhanced crystallite size, but at a certain composition (Ni:N = 2.5; 5) a decline in the average size of crystallites.

TABLE-1
CRYSTALLITE SIZE Ni-N-TiO_2 PHOTOCATALYST

Photocatalyst	Content ratio % mol Ni:N	Average size of crystallites (nm)
Ni-N-TiO_2	2.5:2.5	19.09
Ni-N-TiO_2	5.0:2.5	19.98
Ni-N-TiO_2	10:2.5	33.31
Ni-N-TiO_2	2.5:5.0	23.75
Ni-N-TiO_2	2.5:10	17,23
TiO_2	–	13.12

Diffuse reflection UV spectra: Fig. 4 demonstrate the UV-visible diffuse reflection spectra of TiO_2 photocatalyst doped Ni and or N with composition varied. To determine the band gap energy of photocatalyst used Kubelka Munk equation:

$$\alpha h\nu = A(h\nu - E_g)^n \quad (3)$$

In this equation, A is a constant, α is the coefficient absorption and n = 1/2 for direct transition. The amount of rank n depending on the type of transition that occurs, can be valuable 1/2, 2, 3/2 and 3, respectively associated with the transition direct, indirect, prohibited direct, indirect, forbidden [23].

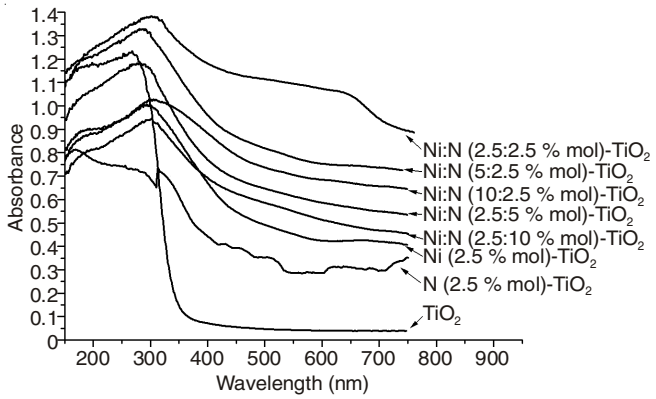

Fig. 4. UV-visible diffuse reflection spectra of pure TiO_2, N-TiO_2, Ni-TiO_2 and Ni-N-TiO_2 samples

Value is determined by the band gap energy photocatalyst plotting $(\alpha h\nu)^2$ as the y-axis *versus* hν as the x-axis. The band gap energy value photocatalyst samples obtained from the intersection of the curve formed by the x-axis.

For a single doping Ni and N in TiO_2 with a concentration of 2.5 mol %, respectively yield band gap energy successively 3.182 and 3.132 eV. This value is lower than the band gap energy of TiO_2 anatase (3.201 eV), which means that with the addition of dopants Ni causes a decrease in the band gap energy of TiO_2. A decrease suspected due to the band gap energy Ni dopant ions that enter into the structure of TiO_2. Therefore, both dopants are individually able to reduce the band gap energy of TiO_2 anatase, then the addition of dual dopant Ni and N in TiO_2 on some variation of the concentration (mol %) by the same method as a single doping Ni and N. Table-2 presented the value of the band gap energy Ni and N co-doped TiO_2 photocatalyst with some variation of the ratio of mol %.

TABLE-2
BAND GAP ENERGY AND λ TiO_2 CO-DOPED Ni AND N

Photocatalyst samples	Ratio % mol Ni:N	Band gap energy (eV)	λ (nm)
Ni-N-TiO_2	2.5:2.5	2.928	422.366
Ni-N-TiO_2	5.0:2.5	3.187	388.039
Ni-N-TiO_2	10:2.5	3.241	381.573
Ni-N-TiO_2	2.5:5.0	3.112	397.390
Ni-N-TiO_2	2.5:10	3.149	392.721
N-TiO_2	2.5	3.093	401.921
N-TiO_2	5	3.132	396.904
N-TiO_2	10	3.151	394.541
Ni-TiO_2	2.5	3.080	403.648
Ni-TiO_2	5	3.182	390.690
Ni-TiO_2	10	3.192	389.457
TiO_2	-	3.201	386.344

If the band gap energy of pure TiO_2 and Ni and N co-doped TiO_2 are compared, it appears that there is a trend decreasing of the band gap energy for the overall sample apart to the sample with a composition ratio (% mol) of Ni:N = 10:2.5. This shows that the doping N direct reduction the band gap energy of TiO_2 so it can respond to visible light, while doping with Ni is not the case. The results turned out to be consistent with the research that has been conducted by Zhang and Liu [3].

SEM-EDX characterization: Fig. 5 shows the results of SEM image of Ni and N co-doped TiO_2 photocatalyst with concentrations 2.5 % mol, respectively. Based on Fig. 5 appears the uniformity of the surface morphology and shape of TiO_2 solids before and after doped with Ni and or N. However, there are differences in changes in the size of TiO_2 solids. Before doped with Ni and N, solids size is relatively small and after the addition dopants Ni and N in general seem to an increase in particle size. It is presumed that this is due to the sintering process with the inclusion of dopants [24]. This fact corresponds to an increase in the size of the previous TiO_2 crystallites have an average size of 13.12 nm and after doped with Ni and N average size of crystallites more than 13.12 nm (Table-1). Not at all the Ni inserted into the TiO_2 structure synthesized *via* sol-gel process can be include TiO_2 structure. EDX analysis shows that in TiO_2 doped Ni photocatalyst with concentration Ni 2.5 % mol, in fact only 1.73 mol % Ni metal which succeed to get into the structure of TiO_2. By ionic radius of Ni^{2+} similar to Ti^{4+}, the Ni^{2+} ionic should have been easily make substitutions to Ti^{4+}. Nevertheless the fact that only about 70 % achievement of Ni into the TiO_2 structure, indicating other factors were responsible for the inclusion of dopant Ni. In another section, the TiO_2 doped N 2.5 % mol, the EDX analysis results do not indicate the presence of N content that inserted into TiO_2 structure. This is presumably because the amount of N added mole percent too small. Zhang *et al.* [17] reported that the addition of dopants N into the system TiO_2 photocatalyst into composite N-TiO_2 has a difficult obstacle produce catalysts with high N concentration.

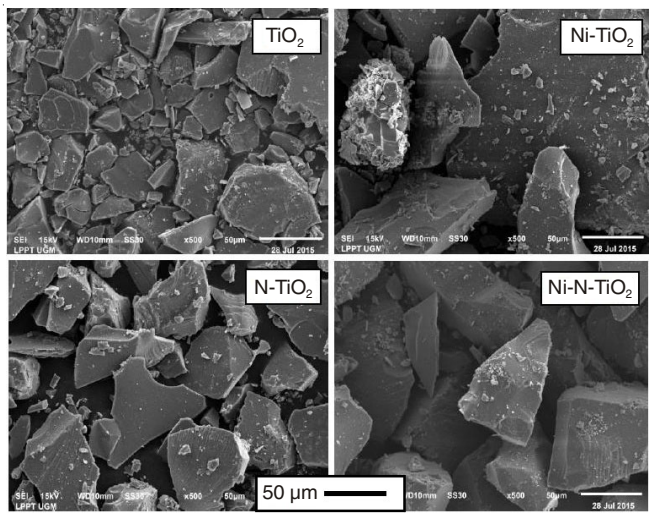

Fig. 5. SEM images of TiO_2 material doped N and N with a composition of 2.5 % mol and calcined at 400 °C

FTIR characterization: The FTIR analysis identify the indications of the bond formation between Ti both Ni and N. The results of FTIR characterization of Ni-TiO_2, N-TiO_2 and Ni-N-TiO_2 potocatalyst is presented in Fig. 6. The functional groups of TiO_2 present in the region of 540 and 690 cm^{-1}. The main uptake appears on FTIR spectra at 900-500 cm^{-1} which is specific absorption in TiO_2 material. Absorption band at 3448 cm^{-1} region is stretching vibration of the O-H owned Ti-OH, whereas the absorption at 1635 cm^{-1} region is O-H bending vibrations are owned H_2O are absorbed on the surface photocatalyst material [25].

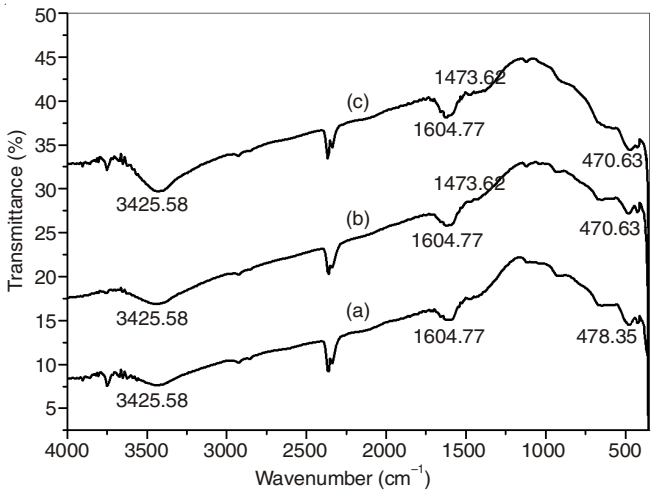

Fig. 6. FTIR spectra of Ni-TiO_2 (a); N-TiO_2 (b); Ni-N-TiO_2 (c) photocatalyst

FTIR spectra in Fig. 6(a) provide different absorption areas on infrared spectra, but did not indicate any new absorption. Uptake of Ti-O stretching vibration that is doped Ni on TiO_2 is 500 cm^{-1}, undergo a shift toward smaller wave numbers. This shift is expected to occur due to the formation of Ti-O bond-Ni. Ti-O bond-Ni has a lower vibration than the vibration Ti-O-Ti. This difference occurs due to ionic radii Ni^{2+} and Ti^{4+} are slightly different. FTIR spectra in Fig. 6(b) shows the main absorption in the region 900-540 cm^{-1} which is a Ti-O stretching vibration. Absorption band at 3448 cm^{-1} region is O-H stretching vibration owned Ti-OH bonds and absorption at 1635 cm^{-1} region is O-H bending vibrations are due to H_2O which absorbed on the surface photocatalyst. In the N-TiO_2 photocatalyst, Ti-O bond vibration undergo a shift toward smaller wave numbers. This is made possible due to the formation of bonds O-Ti-N on N-TiO_2 material. Absorption peaks in the wavelength range of 600-400 cm^{-1} is an absorption peak for bonding Ti-O-Ti and the absorption peak area Ti-N bond. The indication of N-O bond absorption peak in the wavelength range 1550-1200 cm^{-1} [25]. FTIR spectra for N-TiO_2 of this study appear absorption peak at 470.63 cm^{-1} which is the peak for the Ti-N. The presence of a peak at 1442.75 cm^{-1} and 1473.62 cm^{-1} indicate the presence of N-O component. FTIR spectra of TiO_2 co-doped Ni and N presented in Fig. 6(c). Based on Fig. 6(c) shows that the main absorption in the region 900-500 cm^{-1} which is a Ti-O stretching vibration on TiO_2. Absorption band at 3448 cm^{-1} region is O-H stretching vibration owned Ti-OH bonds and absorption at 1635 cm^{-1} region is O-H bending vibrations are due to H_2O. Absorption band at 1473.62 cm^{-1} and 407.63 cm^{-1} are spectra of Ti-N and N-O. As in material Ni-TiO_2 and N-TiO_2, the effect of the addition of Ni and N cause a shift toward smaller wave numbers. This happens because the inception of bonding Ti-Ni-O and O-Ti-N. Uptake shift TiO_2 cause crystal defects or deformation in the crystal structure of TiO_2, so the intensity anatase also decreased [26].

Photocatalytic activity in degradation of methylene blue: Degradation of methylene blue begins with the stage of absorption of photons by the photocatalyst. If the photon energy of the radiation corresponding photocatalysts or exceeds the band gap energy of photocatalyst, the electrons in the valence band of the photocatalyst (O2p) will be excited into the conduction band (Ti3d) produces pairs of holes (h^+_{VB}) and electrons (e^-_{CB}). These electrons then react with O_2 molecules on the surface of TiO_2 form anion, while the hole will react with H_2O molecules produces H^+ ions and $OH^\bullet$ radicals. The $OH^\bullet$ radicals is a very strong oxidizing agent that is able to degrade Methylene blue to species that are not dangerous. The following is the approximate degradation mechanisms as proposed by Houas *et al*. [27], Gokakakar & Salker [28] and Bassaki *et al*. [24].

$$TiO_2 + h\nu \longrightarrow h^+_{VB} + e^-_{CB} \quad (1)$$

$$O_{2(ads)} + e^-_{CB} \longrightarrow O_2^{\bullet-} \quad (2)$$

$$(H_2O \rightarrow H^+ + OH^-)_{ads} + h^+_{VB} \longrightarrow H^+ + OH^\bullet \quad (3)$$

$$O_2^{\bullet-} + H^+ \longrightarrow HO_2^{\bullet-} \quad (4)$$

$$2HO_2^{\bullet-} \longrightarrow H_2O_2 + O_2 \quad (5)$$

$$H_2O_2 + h\nu \longrightarrow 2OH^\bullet \quad (6)$$

$$OH^\bullet + C_{16}H_{18}N_3SCl + 23O_2 \longrightarrow 16CO_2 + 5H_2O + SO_4^{2-} + NH_4^+ + 2NO_3^- + Cl^- + 4H^+ \quad (7)$$

Fig. 7 demonstrates performance of photocatalysts samples on degradating methylene blue. The degree of degradation of photocatalyst increases with the duration of the irradiation used. Long exposure time in a long degradation process illustrates the interaction between photocatalyst with light and the contact between the methylene blue with $OH^\bullet$ radicals. The longer the exposure time, the more energy the photons absorbed by the photocatalyst, so radical $OH^\bullet$ formed on the surface of the photocatalyst more. Moreover, the longer the exposure time means the contact time between the solution on methylene blue with the longer photocatalysts.

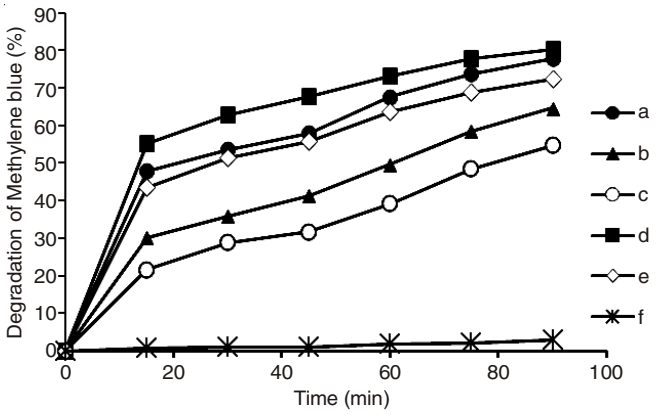

Fig. 7. Performance of TiO_2 co-doped Ni and N photocatalyst in degrading of Methylene blue. The ratio composition (mol %) of Ni:N = 2.5: 2.5 (a); 2.5: 5 (b); 2,5: 10 (c); 5: 2.5 (d); 10: 2.5 (e)

Results of testing the photocatalytic activity of the overall sample of TiO_2 photocatalyst doped with Ni and or N indicate that the degradation of the methylene blue produced by TiO_2 photocatalyst with ratio % mol composition Ni:N = 2.5: 2.5 which is equal to 80.24 % in the 90th min. If the TiO_2 photocatalyst doped with Ni and or N compared it appears that, the photocatalyst has the lowest energy band gap energy (Table-2) and a relatively low particle size (Table-1). This means that the synergy between the width of the band gap energy of photo-

catalyst and crystallite size plays an important role in degradation of methylene blue.

Conclusion

Ni and N co-doped TiO_2 photocatalyst can be synthesized by sol-gel method. The addition of double dopant Ni and N in TiO_2 structure has changed the characteristics of TiO_2, *i.e.* crystallinity, crystallite size and the band gap energy. The addition concentration N (at fixed concentrations of Ni) a greater influence on crystallinity of TiO_2 photocatalyst than the increase in the concentration of Ni (at fixed concentration of N). Increasing calcination temperature increase the average size of crystallites 8.48 nm; 12.1 nm and 14.18 nm, respectively. The addition of dopants Ni and N in TiO_2 photocatalyst in general raise crystallite size, presumably this is due to the sintering process with the inclusion of dopants. This fact corresponds to an increase in the size of the previous TiO_2 crystallites have an average size of 13.12 nm, then after doped with Ni and N the average size of crystallite more than 13.12 nm. In the TiO_2 co-doped Ni and N, increase concentration of Ni (at fixed concentration of N), causing an increase in crystallite size. While on increase concentration N (at fixed concentrations of Ni) initially provides enhanced crystallite size and reaches a maximum at the composition mol % Ni:N = 2.5: 5, then declined. The addition of a single dopant Ni and N decrease the band gap energy of TiO_2 photocatalyst material. The addition of dual dopant Ni and N are generally lowers the band gap energy of TiO_2 with the lowest band gap energy is 2.928 eV achieved by TiO_2 co-doped Ni and N at ratio mol % composition Ni:N = 2.5:2.5. These results also show that doping N direct reduction the band gap energy of TiO_2 so it can respond to visible light, while doping with Ni is not the case. Results of characterization by SEM-EDX showed porous surfaces, rough and form a certain pattern. FTIR characterization results showed that absorption in the region 900-500 cm^{-1} which is a Ti-O stretching vibration and the region of 407.63 and 1473.62 cm^{-1} which is the spectra of the Ti-N and NO. The test results overall sample photocatalytic activity of TiO_2 photocatalyst doped Ni and or N indicate that the rate of degradation of the methylene blue produced by TiO_2 photocatalyst with ratio mol % composition Ni:N = 2.5:2.5 which is equal to 80.24 % in the 90th min. In fact, when this photocatalyst is compared with another TiO_2 photocatalyst doped Ni and or N show the lowest energy band gap energy. This means that the width of the band gap energy of the photocatalyst play an important role in degradation of methylene blue.

ACKNOWLEDGEMENTS

The authors thank for the support from Directorate of Research and Community Service Ministry of Research, Technology and Higher Education (Contract No. 023.04.1.673453/2015 DIPA DIPA dated 14 November 2014 Revision 01 Date March 3, 2015).

REFERENCES

1. K. Hashimoto, H. Irie and A. Fujishima, *AAPS Bull.*, **17**, 6 (2007).
2. X. Zhang and Q. Liu, *Appl. Surf. Sci.*, **254**, 4780 (2008).
3. H. Yan, X. Wang, M. Yao and X. Yao, *Prog. Nat. Sci: Mater. Int.*, **23**, 402 (2013).
4. C. Su, B.-Y. Hong and C.-M. Tseng, *Catal. Today*, **96**, 119 (2004).
5. J. Schneider, M. Matsuoka, M. Takeuchi, J. Zhang, Y. Horiuchi, M. Anpo and D.W. Bahnemann, *Chem. Rev.*, **114**, 9919 (2014).
6. U. Diebold, *Surf. Sci. Rep.*, **48**, 53 (2003).
7. X. Chen and S. Mao, *Chem. Rev.*, **107**, 2891 (2007).
8. M. Ni, M.K.H. Leung, D.Y.C. Leung and K. Sumathy, *Renew. Sustain. Energy Rev.*, **11**, 401 (2007).
9. D.I. Patsoura, X.E. Kondarides and X.E. Verykios, *Appl. Catal. B*, **64**, 171 (2006).
10. M. Anpo and M. Takeuchi, *J. Catal.*, **216**, 505 (2003).
11. Y. Cao, W. Yang, W. Zhang, G. Liu and P. Yue, *New J. Chem.*, **28**, 218 (2004).
12. J. Choi, H. Park and M.R. Hoffmann, *J. Phys. Chem. C*, **114**, 783 (2010).
13. P. Hermawan, H.D. Pranowo and I. Kartini, *Indo. J. Chem.*, **11**, 135 (2011).
14. B. Viswanathan and K.R. Krishanmurthy, *Int. J. Photoenergy*, **2012**, 1 (2012).
15. I. Ganesh, A.K. Gupta, P.P. Kumar, P.S.C. Sekhar, G. Phadmanabhan, K. Radha and G. Sundararajan, *Scientific World J.*, **Article ID 127326** (2011).
16. S. Chin, E. Park, M. Kim and J. Jurng, *J. Powder Technol.*, **201**, 171 (2010).
17. J. Zhang, Y. Wu, M. Xing, S.A.K. Leghari and S. Sajjad, *Energy Environ. Sci.*, **3**, 715 (2010).
18. C. Di Valentin, G. Pacchioni and A. Selloni, *Phys. Rev. B*, **70**, 085116 (2004).
19. T.B. Nguyen, M.J. Hwang and K.S. Ryu, *Bull. Korean Chem. Soc.*, **33**, 243 (2012).
20. M.S. Ghamsari, S. Radiman, M.A.A. Hamid, S. Mahshid and S. Rahmani, *Mater. Lett.*, **92**, 287 (2013).
21. J. Krysa, M. Keppert, J. Jirkovsky, V. Stengl and J. Subrt, *Mater. Chem. Phys.*, **86**, 333 (2004).
22. J. Chen, N. Yao, R. Wang and J. Zhang, *Chem. Eng. J.*, **148**, 164 (2009).
23. J.I. Pankove, Optical Process in Semiconductors, Prentice-Hall Inc., Englewood Cliffs, New Jersey (1971).
24. S. Bassaki, H. Niazi, F. Golestani-Fard, R. Naghizadeh and R. Bayati, *J. Mater. Sci. Technol.*, **31**, 355 (2015).
25. R. Beranek and H. Kisch, *Photochem. Photobiol. Sci.*, **7**, 40 (2008).
26. C.-C. Yen, D.-Y. Wang, L.-S. Chang and H.C. Shih, *J. Solid State Chem.*, **184**, 2053 (2011).
27. A. Houas, H. Lachheb, M. Ksibi, E. Elaloui, C. Guillard and J.-M. Herrmann, *Appl. Catal. B*, **31**, 145 (2001).
28. S.D. Gokakakar and A.V. Salker, *Indian J. Chem. Technol.*, **16**, 492 (2009).